A Functional Role for Tyrosine-D in Assembly of the Inorganic Core of the Water Oxidase Complex of Photosystem II and the Kinetics of Water Oxidation †

ARTICLE *in* BIOCHEMISTRY · JANUARY 2002

Impact Factor: 3.02 · DOI: 10.1021/bi011528z · Source: PubMed

4 AUTHORS, INCLUDING:

Gennady M. Ananyev
Rutgers, The State University of New Jersey
63 PUBLICATIONS **2,060** CITATIONS
SEE PROFILE

Iffet Sakiyan
Ankara University
23 PUBLICATIONS **138** CITATIONS
SEE PROFILE

Gerard Charles Dismukes
Rutgers, The State University of New Jersey
222 PUBLICATIONS **9,075** CITATIONS
SEE PROFILE

A Functional Role for Tyrosine-D in Assembly of the Inorganic Core of the Water Oxidase Complex of Photosystem II and the Kinetics of Water Oxidation†

G. M. Ananyev,‡,§ I. Sakiyan,‡,|| B. A. Diner,⊥ and G. C. Dismukes*,‡

Department of Chemistry, H. Hoyt Laboratory, Princeton University, Princeton, New Jersey 08544, and Central Research and Development Department, Experimental Station, E. I. du Pont de Nemours & Company, Wilmington, Delaware 19880-0173

Received July 23, 2001; Revised Manuscript Received November 13, 2001

ABSTRACT: The role of D2-Tyr160 (Y_D), a photooxidizable residue in the D2 reaction center polypeptide of photosystem II (PSII), was investigated in both wild type and a mutant strain (D2-Tyr160Phe) in which phenylalanine replaces Y_D in the cyanobacterium *Synechocystis sp.* (strain PCC 6803). Y_D is the symmetry-related tyrosine that is homologous to the essential photoactive Tyr161(Y_Z) of the D1 polypeptide of PSII. We compared the flash-induced yield of O_2 in intact, functional PSII centers from both wild-type and mutant PSII core complexes. The yield of O_2 in the intact holo-enzyme was found to be identical in the mutant and wild-type PSII cores using long (saturating) pulses or continuous illumination, but was observed to be appreciably reduced in the mutant using short (nonsaturating) light pulses (<50 ms). We also compared the rates of the first two kinetically resolved steps of photoactivation. Photoactivation is the assembly process for binding of the inorganic cofactors to the apo-water oxidation/PSII complex (apo-WOC−PSII) and their light-induced photooxidation to form the functional $Mn_4Ca_1Cl_x$ core required for O_2 evolution. We show that the D2-Tyr160Phe mutant cores can assemble a functional WOC from the free inorganic cofactors, but at a much slower rate and with reduced quantum efficiency vs wild-type PSII cores. Both of these observations imply that the presence of $Y_D^{\bullet}$ leads to a more efficient photooxidation of the Mn cluster relative to deactivation (reductive processes). One possible explanation for this behavior is that the phenolic proton on Y_D is retained within the reaction center following Y_D oxidation. The positive charge, likely shared by D2-His189 and other residues, raises the reduction potential of P_{680}^+/P_{680}, thereby increasing the driving force for the oxidation of Mn_4Y_Z. There is, therefore, a competitive advantage to organisms that retain the Y_D residue, possibly explaining its retention in all sequences of psbD (encoding the D2 polypeptide) known to date. We also find that the sequence of metal binding steps during assembly of apo-WOC−PSII centers in cyanobacteria cores differs from that in higher plants. This is seen by a reduced calcium affinity at its effector site and reduced competition for binding to the Mn(II) site, resulting in acceleration of the initial lagtime by Ca^{2+}, in contrast to retardation in spinach. Ca^{2+} binding to its effector site promotes the stability of the photointermediates (IM1 and above) by suppressing unproductive decay.

The PSII[1] reaction center protein complex of oxygenic photosynthesis contains two redox-active tyrosines, designated Y_Z and Y_D, each of which can act as an electron donor to the photooxidized primary chlorophyll donor, P_{680}^+, but with greatly different kinetics. These tyrosine residues are located in homologous positions on the third trans-membrane-helix of each of the two homologous polypeptides D1 and D2 that comprise the PSII reaction center (*1*−*5*). Y_Z is rapidly (≤1 μs) oxidized by P_{680}^+ and is rereduced in turn by electrons coming from the tetra-manganese cluster of the WOC during normal PSII turnover. Y_Z has been identified by site-directed mutagenesis as Tyr161 of the D1 polypeptide (*1, 4*). Y_D has been identified as Tyr160 of the D2 polypeptide (*1, 3, 5*). Y_D has been shown by spectroscopic, molecular modeling, and mutagenesis studies to give up its phenolic proton, upon photooxidation to D2-His189, forming a neutral H-bonded radical which persists in the dark (*6, 7*). The role of Y_D has remained unclear. Studies of several site-directed mutants at D2-Tyr160 found that cells grow at 3−4-

† We are grateful to the National Institutes of Health for research support (GM39932). I.S. acknowledges a NATO fellowship supported by TUBITAK (The Scientific and Technical Research Council of Turkey). B.A.D. gratefully acknowledges the support of the NRI/CGP/USDA (97-35306-4882).

* To whom correspondence should be addressed. Voice: 609-258-3949; Fax: 609-258-1980; E-mail: dismukes@princeton.edu.

‡ Princeton University.

§ Present address: Institute of Marine and Coastal Sciences, Rutgers University, 71 Dudley Rd., New Brunswick, NJ 08901.

|| Present address: Department of Chemistry, Ankara University, 06100-Tandogan-Ankara, Turkey.

⊥ E. I. du Pont de Nemours & Company.

[1] Abbreviations: LED, light-emitting diode; P_{680}, primary electron donor; PSII, photosystem II; Q_A and Q_B, primary and secondary plastoquinone electron acceptors of PSII; RC, reaction center; t_{lag}, pre-steady-state lag phase of pulsed-light photoactivation of O_2 evolution; $t_{1/2}$, half-time kinetics of pulsed-light photoactivation of O_2 evolution; Y_{400}, maximal yield of O_2 evolution in the end of photoactivation by 400 flashes; WOC, water oxidizing complex; WT, wild type; Y_Z, redox-active Tyr161 of D1; Y_D, redox-active Tyr160 in the D2 polypeptide, an accessory electron donor to P_{680}^+.

10.1021/bi011528z CCC: $22.00
Published on Web 12/20/2001

fold slower photoautotrophic rates (*1, 10*). In vitro studies of isolated PSII complexes have implicated the $Y_D^{\bullet}$ radical in two reactions: a slow or inefficient oxidation process of the manganese cluster in the holo-enzyme, thereby converting the S_0 state to the S_1 state in the dark under special circumstances, and in its reduced state, shortening the lifetime of the S_2 and S_3 states (*11*−*13*). Results from in vivo photoactivation of whole cells of *Chlamydomonas reinhardtii* suggest that stable photooxidation of Y_D may occur before assembly of the Mn cluster (*14, 15*) and possibly following a light-induced conformational change in the PSII reaction center on the acceptor side between Q_A^- and Q_B, as suggested by previous electrochemical data (*16*).

Photoactivation involves the assembly of a functional WOC from the apo-PSII complex and inorganic cofactors (Mn^{2+}, Ca^{2+}, and Cl^-). The requirement for both light and dark steps for efficient photoactivation in vitro has led to a two-step model for assembly of the cluster, involving sequential light and dark steps of Mn ligation and photooxidation (*17*). Herein, we examine the kinetics and yield of in vitro photoactivation of the WOC in the D2-Tyr160F mutant of *Synechocystis* PCC 6803 cyanobacteria using an ultrasensitive O_2 electrode. Previous work on the native enzyme isolated from spinach has kinetically resolved the first two steps of this process and the specific steps at which Ca^{2+} and Mn^{2+} are taken up (*18*−*20*). Additional studies have examined the specificity for some metal ion inhibitors at these sites (*20, 21*) and the PSII core polypeptide requirements (*22*).

The present results show that the D2-Tyr160Phe mutant can assemble a functional WOC to the same extent as WT PSII but with much slower kinetics and reduced quantum efficiency. These observations suggest that the $Y_D^{\bullet}$ radical promotes more rapid photoactivation of the Mn_4Ca_1 core during assembly and, in the intact holo-enzyme, increases the quantum yield for O_2 formation at low light intensity. We suggest that the origin of both of these observations may be due to an increase in the reduction potential of the primary oxidant P_{680}^+/P_{680} through interaction with the $Y_D^{\bullet}$ radical.

MATERIALS AND METHODS

O_2-evolving PSII core complexes from both the WT and the Y_D-less strain (D2-Tyr160Phe) of the cyanobacterium *Synechocystis sp.* PCC 6803 were prepared as a described by Tang and Diner (*23*). The samples were stored at −196 °C in the assay medium (300 mM sucrose, 35 mM NaCl, 25 mM MES/NaOH buffer, pH 6.0) at a concentration of 0.25−0.75 mg of Chl/mL until used. Manganese-depleted PSII core complexes from *Synechocystis* 6803 both WT and the Y_D-less mutant were prepared by treating with 1.7 mM NH_2OH dissolved in the standard assay medium (*35*). The total incubation time with NH_2OH was 32 min. Excess NH_2-OH was removed by centrifugation at 5000*g* using a Millipore ultrafiltration cell (100 kDa cutoff molecular mass) and washed in assay medium 4 times and stored at −80 °C. The NH_2OH concentration in the medium was reduced by 160 000 times by washing 4 times. No oxygen-evolving activity could be detected after this treatment (measured in the presence of 1.6 mM K_3FeCN_6 and 20 mM $CaCl_2$), confirming the complete removal of functional manganese (*19, 24*). For comparison, we found that residual NH_2OH at 5 μM leads to 50% inhibition of the photoactivation yield using apo-PSII membranes from spinach. All photoactivation experiments were conducted in the standard assay medium containing 1.6 mM K_3FeCN_6 as an electron acceptor, 50 μg of Chl/mL (ca. 1 μM apo-WOC−PSII), as well as $MnCl_2$ and $CaCl_2$ at the concentrations indicated in the text or figure legends.

Photoactivation and detection of O_2 were performed simultaneously in a home-built microcell as described earlier (*19, 24*). The cell characteristics include a 5 μL active volume, a 100 ms time constant, and a sensitivity of 50 fmol of O_2. The cell was illuminated using an ultra bright LED with a wavelength maximum of 660 nm and a peak intensity of $I_p = 80$ mW/cm^2 at 5 mm distance, allowing for flash duration in the range from 1 ms to continuous light. In the present work, the pulsed light parameters were as indicated in the figure legends. The individual light pulses were incremented in duration using a computer program based on LabView (National Instruments). This enabled control of the light pulse duration, shape, and intensity. By using progressively longer square pulses (5−205 ms in 0.5 ms steps), the exponential rise in O_2 yield that occurs during photoactivation with fixed duration pulses is converted to a more linear rise in yield as seen in WT sample in Figure 1. This "scanning pulse width" mode has several advantages: (1) the shorter pulses during the initial phase prior to Mn^{2+} binding reduce the extent of photoinhibition; (2) the systematic error arising from baseline offset due to the LED flash artifact is reduced in the early phase where the signal is weakest; hence, the working sensitivity is improved further; (3) it creates a linearly increasing O_2 signal during the rate-limiting phase of photoactivation if it is governed by a single-exponential process. This permits a linear graphical extrapolation of the rate-limiting slope to obtain a more accurate visual measure of the initial lag phase (*x*-axis intercept at zero O_2 yield) (*25*). Using this method, we previously were able to suppress photoinactivation and detect assembly of a functional WOC in PSII subcore complexes that were very sensitive to photodamage (*22*).

RESULTS

The Flash Yield for O_2 Production in the Intact WOC. Figure 1A demonstrates the time dependence of O_2 evolution produced by a train of 400 light pulses in intact (as isolated) PSII core complexes from WT *Synechocystis sp.* at increasing flash duration from 5 to 205 ms (1st−400th pulse, respectively). Figure 1B shows the corresponding data for the intact PSII cores from the Y_D-less mutant (D2-Tyr160Phe). The O_2 yield produced using long pulses starts to saturate above 50 ms duration, reaching 90% and 63% saturation at 105 ms for WT and the mutant cores, respectively, and becomes independent of flash duration above ca. 175 ms. However, in the early stages of the illumination, when shorter (non-saturating) pulses are used (5 ms initial), there is a much lower O_2 yield in the mutant PSII cores than in WT PSII cores. This arises because under short-pulse illumination the S-state turnover is not limited by the reoxidation of Q_A^-, while under long-pulse illumination photoaccumulation of Q_A^- occurs and limits the flash yield of O_2. This lower O_2 yield in short pulses may arise from an impairment in S-state turnover and/or a lower initial oxidation state in the dark (S_{-1} or lower).

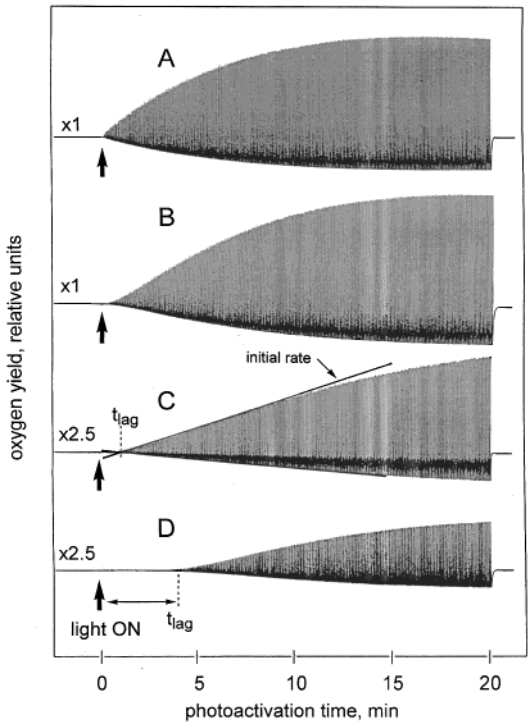

FIGURE 1: Typical experimental trace of the time dependence of oxygen evolution produced by a train of light pulses in PSII core complexes. "Scanning pulse duration method" using 400 light pulses of increasing duration t_{light} = from 5 to 205 ms incremented in steps of 0.5 ms; interpulse dark period, t_{dark} = 3 s. (A) Native PSII cores isolated from WT of *Synechocystis sp.* (strain PCC 6803); (B) native Y_D-less PSII mutant (D2-Tyr160Phe); (C) photoactivation of cofactor-depleted apo-WOC−PSII cores in the presence of inorganic cofactors 200 μM Mn^{2+}/120 mM Ca^{2+}; and (D) photoactivation of the Y_D-less mutant apo-WOC−PSII cores in the presence of inorganic cofactors 200 μM Mn^{2+}/120 mM Ca^{2+}. The flash yield of O_2 under light saturation conditions is the same in the mutant and wild-type samples. Light intensity measured in a continuous mode is 80 mW/cm^2, λ_{max} = 660 nm. Assay conditions: PSII membranes at 50 μg of Chl/mL, 25 mM MES/NaOH buffer (pH 6.0), 35 mM NaCl, 300 mM sucrose, 1.6 mM K_3FeCN_6.

The Kinetics of Photoactivation of Apo-WOC−PSII. Figure 1C presents the time course of photoactivation using WT apo-WOC−PSII cores in the presence of saturating concentrations of the inorganic cofactors (Mn^{2+} and Ca^{2+}), while Figure 1D gives the corresponding data for the Y_D-less apo-WOC−PSII cores under the same conditions. The data show two effects: (1) a 4-fold delay in the onset of recovery of O_2-evolution (lag time) and (2) a 35% slower rate of recovery for the mutant (the initial slope following the lag period). The lag time was determined as the intercept of the extrapolated O_2 yield with the baseline (see figure). A systematic study was undertaken to examine the dependence of the lag time and slope on the concentration of the inorganic cofactors and the dark period.

The kinetics of photoactivation are known to be slowed if the Mn-stabilizing protein that binds to the luminal surface of PSII is not first removed (*35*) or genetically deleted (Psb-O gene) (*36*). We considered unlikely the possibility that the slower kinetics of photoactivation seen in the mutant could arise from preferential retention of the Mn-stabilizing protein vs release from WT cores, following treatment to remove the inorganic cofactors. This interpretation would be in contradiction to previous work by Tamura and Cheniae (*35*) showing that treatment of (spinach) PSII membranes with hydroxylamine releases the extrinsic proteins in proportion to the degree of loss of Mn and O_2 evolution activity. An identical correlation has been observed using alkaline pH treatment (*37*). We found that the single-flash O_2 yield in the intact PSII complexes was equivalent in WT and mutant holo-enzymes, and considered this as evidence for an identical number of active centers. Likewise, the O_2 yields were also equivalent in the WT and mutant apo-WOC− enzymes after completion of photoactivation, although lower, in accordance with expectations based on removal of the extrinsic Mn-stabilizing protein.

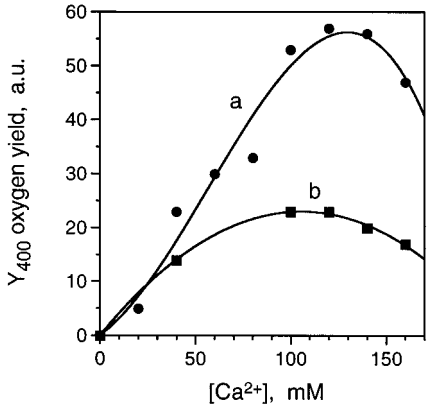

FIGURE 2: Calcium dependence of photoactivation: the O_2 yield produced on the 400th light pulse after reaching a steady state in the number of photoactivated centers (Y_{400}) using excitation by the "scanning pulse duration" method. (a) Apo-WOC−PSII cores from wild-type *Synechocystis* and (b) Y_D-less apo-WOC−PSII mutant core (D2-Tyr160Phe). The medium in Figure 1 was used with 200 μM Mn^{2+}. For other experimental details, see the legend to Figure 1.

Dependence of Photoactivation on $CaCl_2$ Concentration. Figure 2 gives the O_2 yield for WT apo-PSII cores produced on the 400th light pulse (Y_{400}). The concentration profiles for O_2 yield are similar for both WT and the Y_D-less mutant apo-PSII cores (half-saturation at approximately 60 mM in WT vs 30 mM in mutant, peaks at 130 and 100 mM, respectively) and comparable to spinach core complexes (*19*). By contrast, the number of reactivated centers at this point in the photoactivation process is more than 2-fold lower in the mutant vs WT. The lower number of reactivated centers in the mutant after 400 flashes can be recovered if the illumination is continued further. This indicates that the same number of active centers can be restored as in WT apo-PSII cores by providing additional time for the slower photoactivation process to complete in the D2-Tyr160Phe mutant.

Figure 3 gives the duration of the initial lag phase (t_{lag}) on Ca^{2+} concentration. In WT cores, Ca^{2+} is seen to decrease the lag phase continuously from 190 to 15 s between 20 and 150 mM $CaCl_2$, in approximately the same range where the number of active centers also reaches a maximum. Thus, these effects are likely correlated, indicating that the 10-fold acceleration by Ca^{2+} of the first resolvable step leads to a higher population of active centers. This correlation is opposite to that observed in spinach PSII membranes and cores where Ca^{2+} is observed to strongly slow the initial lag phase by 10-fold between 1 and 40 mM Ca^{2+} without decreasing the yield of activatable centers (~100%) (*24*). These data suggest that the initial lag phase in the cyano-

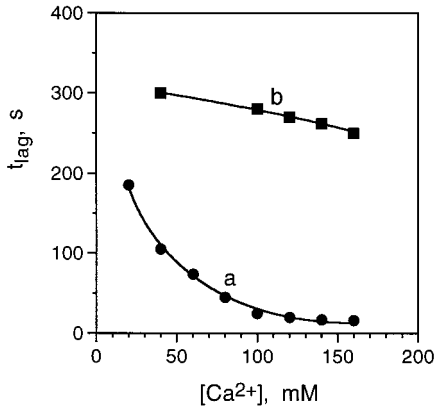

FIGURE 3: Calcium dependence of the photoactivation lag time, defined as the break point in the kinetics of Figure 1 where O_2 evolution begins. (a) Apo-WOC−PSII cores from wild type of *Synechocystis* and (b) Y_D-less apo-WOC−PSII mutant core (D2-Tyr160Phe). Refer to Figure 2 for details.

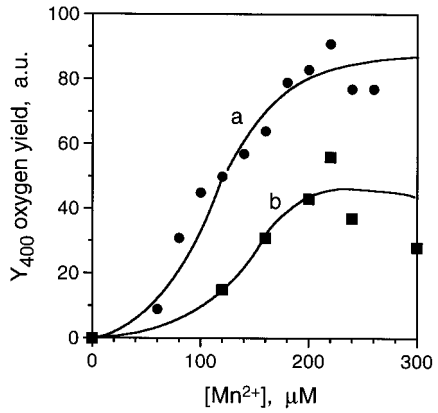

FIGURE 4: Dependence of the number of photoactivated centers (O_2 yield, Y_{400}) in *Synechocystis* apo-WOC−PSII cores on Mn^{2+} concentration. (a) Apo-PSII cores from wild-type *Synechocystis*, $K_m = 108$ μM, and (b) Y_D-less apo-WOC−PSII mutant core (D2-Tyr160Phe), $K_m = 140$ μM. The medium in Figure 1 contains 120 mM Ca^{2+}. For other experimental details, see Figure 1.

bacterial core complexes is measuring a different step or combination of steps than occur prior to the rate-limiting step in the higher plant system. The behavior for the mutant reveals a much longer lag period (305−250 s) and much reduced acceleration by $CaCl_2$ in the same concentration range. The longer lag phase indicates that the D2-Tyr160Phe mutant is impaired in stable photooxidation of Mn^{2+} during photoactivation.

Dependence of Photoactivation on $MnCl_2$ Concentration. Figure 4 shows the dependence on Mn^{2+} concentration of the yield of flash-induced O_2 from photoactivated centers after 400 flashes (Y_{400}) for both WT and the Y_D-less mutant. Figure 5 shows the corresponding data for the lag phase duration. The data were obtained at a fixed concentration of 120 mM Ca^{2+} in the medium, corresponding to the maximum yield seen in Figure 2. The O_2 yield data show that both WT and the mutant reach a maximum at about the same Mn^{2+} concentration (220 μM) and decrease above this concentration; 50% stimulation occurs at about 100 μM Mn^{2+} and about 150 μM for WT and the Y_D-less mutant, respectively. These concentrations are 20−60-fold higher than observed in spinach PSII membranes and cores where concentrations of 4−10 μM Mn^{2+} are sufficient to saturate

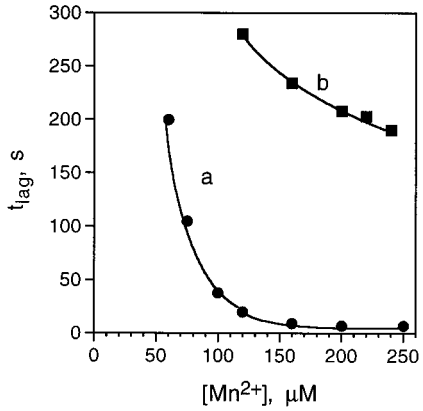

FIGURE 5: Manganese dependence of the photoactivation lag time. (a) Apo-PSII cores from wild-type *Synechocystis* and (b) Y_D-less apo-WOC−PSII mutant core (D2-Tyr160Phe). Refer to Figure 4 for details.

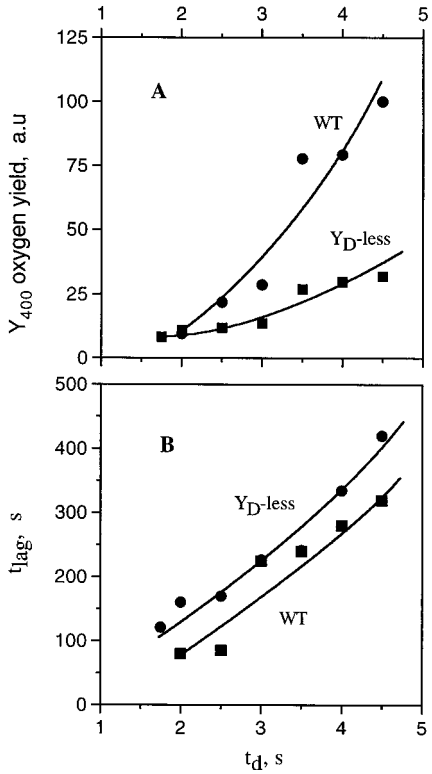

FIGURE 6: Dependence of (A) the number of photoactivated centers (O_2 yield, Y_{400}) and (B) the photoactivation lag time in *Synechocystis* apo-WOC−PSII cores on the duration of the dark period between the light flashes. The "scanning pulse method" was used for excitation. Data for both wild-type and the Y_D-less mutant (D2-Tyr161Phe) are shown. The medium of Figure 1 was used containing 120 mM Ca^{2+}.

the number of active centers. The weaker Mn^{2+} affinity for the *Synechocystis* and *Synechococcus* PSII cores (Watt and Dismukes, unpublished experiments) contrasts with higher plants including spinach, pea, and wheat (*19*, *24*, *25*), suggesting the possibility that weaker Mn^{2+} binding to cyanobacterial apo-WOC−PSII centers vs higher plant apo-WOC−PSII centers may be a general observation. This effect appears not to be due to stronger competition with Ca^{2+} at the high-affinity Mn^{2+} site in the cyanobacteria, as this would result in even greater loss in photoactivation yield with increasing Ca concentration, which is not seen.

Scheme 1: Model of the Sequence of Kinetic Intermediates Formed during Assembly of the Inorganic Core of the WOC by Photoactivation, Including a Role for Tyrosine's Y_Z and Y_D

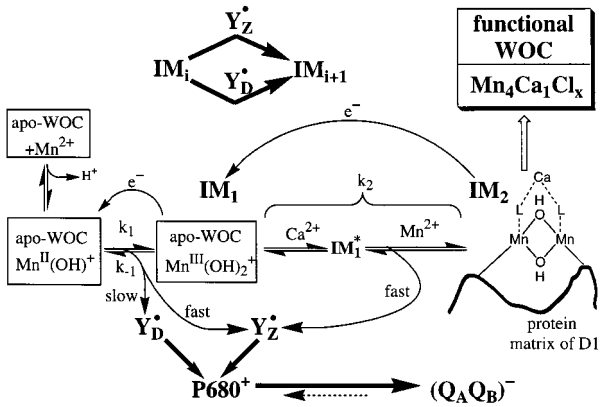

The dependence of the lag phase on $MnCl_2$ concentration, shown in Figure 5, is very similar to the behavior with $CaCl_2$ concentration. In WT PSII cores, an increasing concentration of Mn^{2+} accelerates the lag phase from 200 to <5 s between 20 and 140 μM, and remains <5 s up to 250 μM Mn^{2+}. In the mutant cores, a much longer lag phase is observed, and this is more weakly accelerated by Mn^{2+}, decreasing from 280 s at 100 μM Mn^{2+} to 200 s at 260 μM Mn^{2+}.

Dependence of Photoactivation on the Interpulse Dark Period. To examine the deactivation rate of the flash-induced intermediates, we investigated the dependence of photoactivation yield and lag time on the duration of the dark period between the LED flashes, given in Figure 6 A,B, respectively. The O_2 yield data for WT cores show that the number of photoactivated centers created after 400 pulses (Y_{400}) increases between 1.5 and 4.5 s. The data for the mutant also show an identical yield as WT at short dark intervals but with much lower yields at longer dark intervals. These data indicate that the number of photoactivated centers is limited by one or more slow dark processes that require longer than 4.5 s to complete before the next light flash can be optimally utilized for subsequent photooxidation steps. This trend is true for both WT and the Y_D-less mutant, but with deactivation more effectively offsetting light-driven S-state advance in the mutant. Furthermore, the competing deactivation processes, which contribute to lowering the yield, must have a lifetime that is equal to or greater than the longest dark interval examined; otherwise, the yield would not continue to increase with increasing dark interval.

The lag phase data in Figure 6B show that longer dark intervals between flashes lead to longer lag times for the onset of O_2 evolution, ranging from 75 to 320 s for intervals of 1.8−4.5 s in WT for the particular choice of cofactor concentrations used. The lag times are longer in mutant cores than in WT cores and show no evidence of reaching saturation with increasing dark intervals up to 4.5 s. The lag phase remains shorter in the WT cores than in the Y_D-less mutant cores. A larger difference is observed at higher concentrations of the cofactors as noted previously in Figures 3 and 5. The longer lag times observed as the dark interval increases suggest that deactivation of IM_1 (Scheme 1), that forms upon the first illumination, occurs in both WT and Y_D-less mutant cores. This feature is common to the kinetics seen in earlier work on spinach apo-WOC−PSII (*19, 24*). The longer lag times in Figure 6B (and Figures 3 and 5) for the mutant indicate that the $Y_D^\bullet$ radical contributes to the kinetic stability (lifetime) possibly as early as the first observable intermediate in the assembly process. This amounts to a 2-fold decrease in lifetime relative to WT cores at a dark interval of 2 s between flashes at the cofactor concentrations used in Figure 6B. We estimate the lifetime for this early intermediate in the mutant cores to be less than 2 s based on these data.

DISCUSSION

The data in Figure 1A,B show that under nonsaturating light flux conditions, when infrequent turnover of the donor side reactions (S-state transitions) should control the amount of O_2 produced, an appreciably lower flash yield is observed for the Y_D-less mutant vs WT. This figure shows, however, that the difference in light utilization between PSII core complexes of WT and of the Y_D-less mutant disappears when the duration of the light pulses become longer than 50 ms and turnover of the acceptor side becomes rate-limiting.

There are three possible mechanisms that may contribute to a reduced yield of O_2 in the mutant using short flashes: (1) a smaller optical cross section for the D2-Tyr160Phe mutant compared to WT, (2) the presence of a lower oxidation state in the dark (S_0 or lower) than exists in WT PSII (predominantly S_1), and (3) a lower yield for the oxidation by P_{680}^+ of Mn_4Y_Z in the S_2 and S_3 states, possibly combined with a faster deactivation of the S_2 and S_3 states by recombination (on the order of the 3 s dark period).

The number of chlorophylls per center is the same in the D2-Tyr160Phe core complex as in the WT, making it unlikely that the difference in flash yield arises from a difference in optical cross section. While it is possible that in the fully intact core complexes the Y_D-less complex is present in a more reduced S-state, there is no a priori reason to expect that this would be the case. Furthermore, in Figure 1C,D, the initial state of the mutant and WT core complexes is identical prior to photoactivation. The increased lag time associated with the appearance of oxygen in the mutant complex argues that in both the S-state cycling and the photoactivation there is a decreased quantum yield for the oxidation of Mn associated with the absence of $Y_D^\bullet$.

There are two possible mechanisms for the enhanced quantum yield for the oxidation of Mn in the presence of $Y_D^\bullet$. In the first, $Y_D^\bullet$ could participate as an oxidizing equivalent that can advance an unstable intermediate in the Mn cluster during assembly to a more stable oxidized state. This role would only apply to photoactivation and not to S-state cycling as the reduction potential of $Y_D^\bullet/Y_D$ is too low to drive the oxidation of anything but S0→S1 and the rate for this process is thought to be quite slow (tens of minutes) (*11*). In the second mechanism, the presence of the $Y_D^\bullet$ radical would function to increase the reduction potential of P_{680}^+, thus increasing the equilibrium constant for reduction via the Mn_4Y_Z pathway. An increase in the P_{680}^+ potential could be expected in WT due to a Coulombic interaction between P_{680}^+ and the trapped positive charge created by oxidation of Y_D and its associated hydrogen-bonded base (D2-H^+His189) (*6, 7*). This mechanism would apply to both photoactivation and S-state cycling. In the latter case, the control of the reduction potential of P_{680}^+/P_{680} would

be particularly critical in the S2→S3 and the S3→S4 (S0) transitions where the equilibrium constant for $Sn P_{680}^{+} \leftrightarrow S n^{+1} P_{680}$ has been estimated to be less than 5 (*34*).

The second mechanism is consistent with an observation of Boerner et al. (*27*), who studied the recombination kinetics between Q_A^- and the oxidized donor in Mn-depleted PSII core complexes isolated form WT and the D2-Tyr160Phe mutant. Charge recombination occurs between Q_A^- and P_{680}^+. Consequently, the rate of recombination is determined by the equation: $k_{obs} = k_{in}[Q_A^-][P_{680}^+]$, where k_{obs} is the observed rate of recombination and k_{in} is the intrinsic rate of recombination between P_{680}^+ and Q_A^-. The core complexes do not contain functional Q_B, and so every center in which charge separation has occurred contains Q_A^- immediately following charge separation. The rate of charge recombination is therefore determined by the concentration of P_{680}^+, $[P_{680}^+] = 1/(1 + K_{zp})$, where $K_{zp} = [Y_Z^{\bullet} P_{680}]/[Y_Z P_{680}^+]$ and $k_{obs} = k_{in}/(1 + K_{zp})$. The recombination kinetics observed by Boerner et al. (*27*) were close to 2-fold more rapid in the mutant than in the WT, indicating that K_{zp} is 2-fold larger in the WT than in the mutant. This observation could be explained by an approximate 18 mV increase in the reduction potential of P_{680}^+/P_{680} in the presence of $Y_D^{\bullet}$. The same effect of $Y_D^{\bullet}$ on the reduction potential of P_{680}^+/P_{680} would be expected to occur even in the presence of an intact Mn cluster. We conclude, therefore, that the second mechanism is consistent with the available data, namely, that the hole created by the $Y_D^{\bullet}$ radical appears to promote a higher quantum yield for O_2 production in WT PSII via an increase in the reduction potential of P_{680}^+, thereby increasing the quantum yield of oxidation of $Mn_4Y_Z^{\bullet}$ by P_{680}^+. We do not, however, exclude a possible role for the first mechanism in photoactivation.

The dependence of the relative photoactivation yield (Y400) on the $MnCl_2$ and $CaCl_2$ concentrations is not appreciably different for WT and the Y_D-less mutant (absolute yields do differ), suggesting similar intrinsic binding affinities and comparable inhibition at excess concentrations. By contrast, there is a large difference in their lag time for photoactivation and its concentration dependence on both $CaCl_2$ and $MnCl_2$. The mutant is impaired in generating and stabilizing photointermediates, as seen by the longer lag phase, the slower rate-limiting O_2 recovery phase, and the weaker influence of the dark interval on photoactivation yield. This impairment cannot be overcome merely by increasing the concentration of the inorganic cofactors, which produces a comparatively modest acceleration of the lag period relative to the large acceleration seen in WT cores (Figures 3 and 5). A lower quantum yield for photoactivation and an enhanced sensitivity to reductive losses (deactivation) appear to limit the rate and yield of cluster formation in the Y_D-less mutant at steps that are only modestly affected by the Ca^{2+} and Mn(II) concentrations. In WT, however, these same steps show a much more marked dependence on both cations. Once the Mn cluster is assembled, however, the dependence of O_2 yield on the concentration of Ca^{2+} and Mn(II) is equivalent in WT and the Y_D-less mutant (Figures 2 and 4), indicating that their influence on the assembled Mn cluster is independent of the presence of $Y_D^{\bullet}$.

We present a molecular model to interpret these effects. It is identical to the model we have proposed for interpretation of photoactivation kinetics in higher plants, with an extension to include the role of Y_D (*20*). The $Y_D^{\bullet}$ radical serves two functions. First, a positive hole associated with the retention of the phenolic proton with the reaction center upon Y_D oxidation would be potentially capable of raising the reduction potential of the redox couple $P680^+/P680$ by an electrostatic interaction. This positive charge is likely delocalized between the nearby base thought to be D2-His189 (*6, 7, 10*) and adjacent residues. Second (see Scheme 1), the $Y_D^{\bullet}$ radical is proposed to be capable of contributing its oxidizing equivalent to one of the intermediate oxidation steps in the photoactivation of the Mn cluster. Such an oxidation could allow the assembling Mn cluster to pass rapidly through an unstable state that might otherwise undergo reduction in the absence of $Y_D^{\bullet}$.

Although the nature of the dark processes that occur during photoactivation has not been examined in detail yet for cyanobacterial PSII centers, in spinach it is clearly established that the kinetically limiting dark process involves a slow (>10 s) binding of Ca^{2+} to its effector site, following the formation of the first light-induced intermediate IM1 (Scheme 1) (*31, 32*). IM1 is very likely equivalent to the photooxidized Mn(III) center recently detected using EPR spectroscopy (*33*). The binding of the remaining three Mn^{2+} ions from solution occurs after Ca^{2+} binds in higher plants (*18*). This ordered binding sequence of Mn/Ca/3Mn occurs under conditions of limiting Mn^{2+} concentration because Ca^{2+} binding leads to an increased affinity for the second and subsequent Mn^{2+} ions, which otherwise do not bind with high affinity in the absence of Ca^{2+} (*32*). The data presented here for cyanobacterial PSII do not show kinetic resolution of the first two steps. The effect of calcium on the lag phase is *opposite* to the elongation of the lag phase seen during photoactivation in spinach, where calcium accelerates decay of IM1 by competitive binding to the initial Mn(II) site (*24, 32*). The present data show that both Ca^{2+} and Mn^{2+} bind more weakly and with less competition during the lag phase period prior to O_2 evolution. Calcium is able to stabilize one or more intermediates formed during photoactivation.

The general model in Scheme 1 is able to explain this major difference in the kinetic data of the two organisms. We propose that calcium stabilizes the first manganese photooxidation step in cyanobacteria by binding to its effector site during conversion of IM1 to IM1*. Hence, we would expect to see a rate acceleration through the lag phase upon calcium addition provided that the decay of IM1 induced by Ca^{2+} is a lower probability process in the case of cyanobacteria, than is, calcium binding to its effector site which forms IM1*. Direct evidence for Ca^{2+} stabilizing the binding of the first two Mn(II) ions has been observed in spinach PSII membranes from EPR data (*32*). Analogous evidence for the case of cyanobacterial PSII centers is unavailable to date.

The discussion above indicates that the $Y_D^{\bullet}$ radical serves an important although nonessential role both in the biogenesis of a stable inorganic core during photoactivation of the WOC and in S-state cycling by increasing the flash yield for O_2 production for short light pulses. These functional roles should confer an evolutionary advantage to the retention of the Y_D residue within the D2 polypeptide throughout the evolution of the genome of ancestral organisms and higher plants. Examination of the database of D2 sequences reveals that the Y_D residue has been retained in all sequences

reported thus far (about 52), extending over all known examples of oxygen-producing photosynthetic organisms.

ACKNOWLEDGMENT

We are grateful to a patient reviewer.

REFERENCES

1. Debus, R. J., Barry, B. A., Sithole, I., Babcock, G. T., and McIntosh, L. (1988) *Biochemistry 27*, 9071−9074.
2. Babcock, G. T., and Diner, B. A. (1996) in *Oxygenic Photosynthesis: The Light Reactions* (Ort, D., and Yocum, C., Eds.) pp 213−247, Kluwer, Dordrecht.
3. Barry, B., and Babcock, G. T. (1987) *Proc. Natl. Acad. Sci. U.S.A. 84*, 7099−7103.
4. Metz, J. G., Nixon, P. J., Rögner, M., Brudvig, G. W., and Diner, B. A. (1989) *Biochemistry 28*, 6960−6969.
5. Vermaas, W. F. J., Rutherford, A. W., and Hansson, O. (1988) *Proc. Natl. Acad. Sci. U.S.A. 85*, 8477−8481.
6. Tang, X.-S., Chisholm, D. A., Dismukes, G. C., Brudvig, G. W., and Diner, B. A. (1993) *Biochemistry 32*, 13742−13748.
7. Campbell, K., Peloquin, J., Diner, B., Tang, X.-S., Chisholm, D. A., and Britt, R. (1997) *J. Am. Chem. Soc. 119*, 4787−4788.
8. Hays, A.-M., Vassiliev, I. R., Golbeck, J. H., and Debus, R. J. (1999) *Biochemistry 38*, 11851−11865.
9. Hays, A.-M., Vassiliev, I. R., Golbeck, J. H., and Debus, R. J. (1998) *Biochemistry 37*, 11352−11365.
10. Debus, R. J. (2000) in *Metal Ions in Biological Systems* (Sigel, H., Ed.) pp 657−710, Marcel Dekker, New York.
11. Styring, S., and Rutherford, A. W. (1987) *Biochemistry 26*, 2401−2405.
12. Vass, I., and Styring, S. (1991) *Biochemistry 30*, 830−839.
13. Babcock, G. T., and Sauer, K. (1975) *Biochim. Biophys. Acta 376*, 315−328.
14. Rova, M., Mamedov, F., Magnuson, A., Fredicksson, P.-O., and Styring, S. (1998) *Biochemistry 37*, 11039−11045.
15. Magnuson, A., Rova, M., Mamedov, F., Fredrickson, P.-O., and Styring, S. (1999) *Biochim. Biophys. Acta 141*, 180−191.
16. Johnson, G. N., Rutherford, A. W., and Krieger, A. (1995) *Biochim. Biophys. Acta 1229*, 202−207.
17. Tamura, N., and Cheniae, G. M. (1987) *Biochim. Biophys. Acta 890*, 179−194.
18. Zaltsman, L., Ananyev, G., Bruntrager, E., and Dismukes, G. C. (1997) *Biochemistry 36*, 8914−8922.
19. Ananyev, G. M., and Dismukes, G. C. (1996) *Biochemistry 35*, 4102−4109.
20. Ananyev, G. M., Zaltsman, L., Vasko, C., and Dismukes, G. C. (2001) *Biochim. Biophys. Acta 1503*, 52−68.
21. Ananyev, G. M., Murphy, A., Abe, Y., and Dismukes, G. C. (1999) *Biochemistry 38*, 7200−7209.
22. Büchel, C., Barber, J., Ananyev, G. M., Eshaghi, S., Watt, R., and Dismukes, G. C. (1999) *Proc. Natl. Acad. Sci. U.S.A. 96*, 14288−14293.
23. Tang, X.-S., and Diner, B. A. (1994) *Biochemistry 33*, 4594−4603.
24. Ananyev, G. M., and Dismukes, G. C. (1996) *Biochemistry 35*, 14608−14617.
25. Baranov, S. V., Ananyev, G. M., Klimov, V. V., and Dismukes, G. C. (2000) *Biochemistry 39*, 6060−6065.
26. Vavilin, D. V., and Vermaas, W. F. J. (2000) *Biochemistry 39*, 14831−14838.
27. Boerner, R. J., Bixby, K. A., Nguyen, A. P., Noren, G. H., and Debus, R. J. (1993) *J. Biol. Chem. 268*, 1817−1823.
28. Forbush, B., Kok, B., and McGloin, M. P. (1971) *Photochem. Photobiol. 11*, 457−475.
29. Tang, X.-S., Zheng, M., Chisholm, D. A., Dismukes, G. C., and Diner, B. A. (1996) *Biochemistry 35*, 1475−1484.
30. Chen, C., Kazimir, J., and Cheniae, G. M. (1995) *Biochemistry 34*, 13511−13526.
31. Ananyev, G. M., Zaltsman, L., McInturff, R. A., and Dismukes, G. C. (1998) in *Photosynthesis: Mechanisms and Effects* (Proceedings of the XIth International Photosynthesis Congress) (Garab, G., Ed.) pp 1347−1350, Kluwer, Dordrecht.
32. Ananyev, G. M., and Dismukes, G. C. (1997) *Biochemistry 36*, 11342−11350.
33. Campbell, K. A., Force, D. A., Nixon, P. J., Dole, F., Diner, B. A., and Britt, R. D. (2000) *J. Am. Chem. Soc. 122*, 3754−3761.
34. Shinkarev, V. P., and Wraight, C. (1993) *Photosynth. Res. 38*, 315−321.
35. Tamura, N., and Cheniae, G. (1985) *Biochim. Biophys. Acta 809*, 245−259.
36. Burnap, R. L., Qian, M., and Pierce, C. (1996) *Biochemistry 35*, 874−882.
37. Hunziker, D., Abramowicz, D. A., Damoder, R., and Dismukes, G. C. (1987) *Biochim. Biophys. Acta 890*, 6−14.

BI011528Z